
Proceedings of the Eighteenth International Conference on
Civil, Structural and Environmental Engineering Computing
Edited by: P. Iványi, J. Kruis and B.H.V. Topping
Civil-Comp Conferences, Volume 10, Paper 12.1
Civil-Comp Press, Edinburgh, United Kingdom, 2025
ISSN: 2753-3239, doi: 10.4203/ccc.10.12.1


# Failure Analysis of Quasi-Brittle Materials Using Coupled Refined Finite Elements and Peridynamics Incorporating Cohesive Effects

**A. Pagani[1], J. Shen[1] and M. Rui Arruda[2]**

**[1] Department of Mechanical and Aerospace Engineering, Politecnico di Torino, Turin, Italy**
**[2] Department of Structures, National Laboratory of Civil Engineering, Lisbon, Portugal**

## Abstract

This work investigates the crack propagation and failure behavior of quasi-brittle materials by combining two different numerical models. The critical region, where damage or cracks may occur, is modeled using three-dimensional (3D) bond-based peridynamics (PD). The remaining elastic region is modeled with one-dimensional (1D) higher-order beam elements based on the Carrera Unified Formulation (CUF). The coupling between the two models is achieved through Lagrange multipliers. An improved damage model is proposed in PD to account for the cohesive effects of quasi-brittle materials. In addition, an implicit displacement control method is employed in PD to improve convergence for quasi-brittle failure. The proposed approach is validated through comparison with experimental data. The results show that the model can accurately capture crack propagation and load–displacement curves in an efficient manner.

**Keywords:** finite elements, peridynamics, nonlocal computational models, fracture, coupled local-nonlocal models, damage modelling.

# 1 Introduction

Quasi-brittle materials, such as concrete and composites, are widely used in engineering structures. A reliable numerical method is essential to accurately predict crack propagation and material failure. Over the past decades, many numerical models have been developed based on classical continuum mechanics. However, these models still face several limitations. For example, the smeared crack model suffers from mesh-dependence [1], while the discrete crack model often requires re-meshing during crack growth [2].

Peridynamics (PD), first introduced in [3], is a promising computational method to overcome the limitations of classical continuum mechanics. In PD, the continuous body is discretized into a set of particles, and each particle interacts with others within a certain horizon radius $\delta$. The governing equations are written in an integro-differential form, which allows PD to describe discontinuous displacement fields. PD has been widely applied to simulate various complex failure processes [4].

Apart from the PD formulation itself, accurately modeling damage and failure in quasi-brittle materials remains a challenge. A critical bond-stretch-based criterion was proposed in [5] to describe the failure of brittle materials. However, unlike brittle materials, quasi-brittle materials exhibit significant strain-softening behavior, indicating that cohesive effects exist on crack surfaces after microcracks form. To address this, many studies have proposed damage models in PD that can account for the cohesive effect when simulating the failure of quasi-brittle materials [6, 7].

However, due to its non-local nature, PD often leads to large, sparse, and non-banded system matrices, which result in high computational cost. In addition, the boundary conditions in PD models are difficult to apply, and surface effects may appear because of the non-local interactions. To improve computational efficiency, the finite element method (FEM) can be used in the elastic domain and near the boundaries, while PD grids can be applied in critical regions where damage, cracks, or discontinuities are expected.

Several coupling techniques have been proposed, such as overlapped zone-based methods [8] and shared node-based methods [9]. In [10], a three-dimensional (3D) PD model was coupled with higher-order one-dimenasional (1D) finite elements. This approach improves computational efficiency, as 1D elements are implemented within the Carrera Unified Formulation (CUF) [11], which allows quasi-3D accuracy through expansion functions in the beam model. A similar approach was used in [12] for fracture analysis, where 3D PD was coupled with higher-order beam models. However, the cohesive effect was not considered in that study.

Given the above context, this work proposes a damage model, inspired by [13, 14], for the failure analysis of quasi-brittle materials in PD. A higher-order beam model is also coupled in the elastic domain, as done in [10], to reduce computational cost. Additionally, an implicit displacement control method is adapted from classical mechanics to enhance stability in the softening regime.

## 2 Bond-based peridynamic theory

The bond-based peridynamic (BBPD) model was the first PD formulation proposed in [3]. In the framework of PD, a continuum solid is represented by a collection of material particles with infinitesimal volume $dV$. Each particle at position $\boldsymbol{x}$ interacts with other particles $\boldsymbol{x}'$ located within its horizon $\mathbf{H}_x$, which is defined by a radius $\delta$.

The relative position between two particles is given by the vector $\boldsymbol{\xi} = \boldsymbol{x}' - \boldsymbol{x}$, while the relative displacement is denoted by $\boldsymbol{\eta} = \boldsymbol{u}' - \boldsymbol{u}$, where $\boldsymbol{u}'$ and $\boldsymbol{u}$ are the displacement of particle $\boldsymbol{x}'$ and $\boldsymbol{x}$, respectively.

The interaction force between two particles is described by a pairwise force density function $\boldsymbol{f}$. The static equilibrium equation of a particle $\boldsymbol{x}$ is governed by the following integro-differential equation:

$$\int_{\mathbf{H}_x} f(\boldsymbol{\xi}, \boldsymbol{\eta}) dV_{x'} + \boldsymbol{b}(\boldsymbol{x}) = \mathbf{0} \tag{1}$$

where $\boldsymbol{b}(\boldsymbol{x})$ is the body force density vector.

For isotropic elastic materials, the pairwise force density can be expressed as [3]:

$$\boldsymbol{f}(\boldsymbol{\xi}, \boldsymbol{\eta}) = cs \frac{\boldsymbol{\xi} + \boldsymbol{\eta}}{|\boldsymbol{\xi} + \boldsymbol{\eta}|} \tag{2}$$

with

$$s = \frac{|\boldsymbol{\xi} + \boldsymbol{\eta}| - |\boldsymbol{\xi}|}{|\boldsymbol{\xi}|} \tag{3}$$

$$c = \frac{12E}{\pi \delta^4} \quad \text{for 3D case} \tag{4}$$

where $s$ is the bond stretch, $c$ is the micro-modulus representing the bond stiffness, and $E$ is the elastic modulus.

The PD domain is discretized into a grid of material points or nodes. After discretization, the static equilibrium equation becomes a summation over the family nodes of each point. For node $\boldsymbol{x}_i$, the discrete form is:

$$\sum_{j=1}^{N_{H_i}} \boldsymbol{f}_{ij} V_j + \boldsymbol{b}_i = 0 \tag{5}$$

where $N_{H_i}$ is the number of family nodes of node $\boldsymbol{x}_i$ and $V_j$ is the volume of particle $\boldsymbol{x}_j$.

In a homogeneous material, and after linearization, Eq. (5) can be written in a matrix form:

$$\sum_{j=1}^{N_{H_i}} \boldsymbol{C}(\boldsymbol{x_j} - \boldsymbol{x}_i)(\boldsymbol{u}_j - \boldsymbol{u}_i) V_j + \boldsymbol{b}_i = 0 \tag{6}$$

with

$$\boldsymbol{C}(\boldsymbol{\xi}) = c \frac{\boldsymbol{\xi} \otimes \boldsymbol{\xi}}{|\boldsymbol{\xi}|^3} \tag{7}$$

By multiplying both sides of Eq. (6) by the volume $V_i$, the equilibrium equation becomes suitable for finite element analysis:

$$\sum_{j=1}^{N_{H_i}} \boldsymbol{C}(\boldsymbol{x_j} - \boldsymbol{x}_i)(\boldsymbol{u}_j - \boldsymbol{u}_i)V_i V_j + \boldsymbol{b}_i V_i = 0 \tag{8}$$

or

$$\boldsymbol{K}_{PD}\boldsymbol{U}_{PD} = \boldsymbol{F}_{PD} \tag{9}$$

# 3 Higher-order beam theory

The Carrera Unified Formulation (CUF) [11] is a framework that allows the generation of higher-order beam theories with three-dimensional accuracy and a significant reduction in computational cost. In the CUF framework, the 3D displacement field of a beam model can be written as:

$$\mathbf{u}(x, y, z) = F_\tau(x, z)\mathbf{u}_\tau(y), \quad \tau = 1, 2, ..., M \tag{10}$$

where $\mathbf{u}_\tau(y)$ is the displacement vector; $F_\tau$ are the cross-sectional expansion functions; $\mathbf{u}_\tau$ is the generalized displacement vector; $M$ is the number of terms in the expansion function; The subscript $\tau$ indicates the summation. Common choices for the expansion functions include Taylor and Lagrange polynomials.

The finite element method (FEM) can be used to approximate the generalized displacement vector. Therefore, Eq. (10) can be rewritten as:

$$\mathbf{u}(x, y, z) = F_\tau(x, z)N_i(y)\mathbf{u}_{\tau i}, \quad i = 1, 2, ..., N_n \tag{11}$$

where $N_n$ is the number of nodes for each beam element; $i$ indicates the summation; $N_i$ is the shape function in 1D elements; $\mathbf{u}_{\tau i}$ is the unknown nodal vector.

The governing equations of the CUF-based model can be derived using the Principle of Virtual Displacement (PVD). Details are available in [11]. For static analysis, the governing equation can be expressed as:

$$\mathbf{K}_{\tau sij}\mathbf{u}_{\tau i} = \mathbf{F}_{sj} \tag{12}$$

where $\mathbf{K}_{\tau sij}$ is the $3 \times 3$ fundamental nucleus that can be used to assemble the global stiffness matrix through the looping on four indexes $\tau$, $s$, $i$, and $j$. Moreover, the above governing equation can be compacted as follows:

$$\boldsymbol{K}_{\mathrm{FE}}\boldsymbol{U}_{\mathrm{FE}} = \boldsymbol{F}_{FE} \tag{13}$$

To reduce the high computational cost of peridynamic modeling caused by its nonlocal nature, a CUF-based 1D beam model can be coupled with 3D PD. To enforce the continuity condition at the interface between the PD and 1D finite element domains,

Lagrange multipliers are introduced following the method in [10]. The matrix form of the coupled system is:

$$\begin{bmatrix} \boldsymbol{K} & \boldsymbol{B}^{\mathrm{T}} \\ \boldsymbol{B} & \mathbf{0} \end{bmatrix} \begin{bmatrix} \mathbf{U} \\ \lambda \end{bmatrix} = \begin{bmatrix} \mathbf{F} \\ \mathbf{0} \end{bmatrix} \tag{14}$$

where $\boldsymbol{B}$ is the coupling matrix and $\boldsymbol{K}$ is the global stiffness matrix. $\mathbf{U}$ is the unknown displacement vector and $\lambda$ is the unknown Lagrange multiplier vector.

# 4 Improved damage model for quasi-brittle materials

The bond stretch criterion, introduced in [5], is a common approach for modeling damage, crack propagation, and failure in brittle materials. According to this criterion, a bond is considered broken when the stretch exceeds a critical value $s_c$. However, this approach may not accurately represent the damage mechanism of quasi-brittle materials, which typically exhibit strain-softening behavior.

As discussed in [6], the damage model in peridynamics is conceptually similar to the stress–strain relationship in classical continuum mechanics, where the pairwise force corresponds to stress and the bond stretch corresponds to strain. Based on this idea, a new damage model with a softening law is proposed to replace the traditional linear damage model.

Figure 1 illustrates the proposed model, which is referred from the constitutive laws from [13, 14]. In this model, the bond force increases linearly with stretch until the tensile limit $s_{t0}$ is reached. Beyond this limit, the bond enters a degradation stage governed by an exponential softening function. The expression of the proposed model is given as:

$$f = \begin{cases} cs, & s \le s_0 \\ f_{\max} \exp\left(\frac{s_0 - s}{s_u - s_0}\right), & s > s_0 \end{cases} \tag{15}$$

where $f_{\max} = cs_0$ is the maximum bond pairwise force when the stretch achieves the limit $s_0$. $s_u$ is the ultimate stretch in the case of linear softening and can be computed using the tangent to the exponential softening curve computed as the peak point.

Following the method in [6], it is assumed that the normal stress acting on a plane reaches the tensile strength $f_t$ when all bonds crossing the plane are stretched to $s_0$. Based on this assumption, the stretch limit $s_0$ in the 3D case can be analytically determined by:

$$f_t = \int_0^{\delta} dz \int_0^{2\pi} d\theta \int_z^{\delta} d\xi \int_0^{\cos^{-1}(z/\xi)} cs_0 \cos\phi \xi^2 \sin\phi d\phi \tag{16}$$

and the solution is:

$$s_0 = \frac{6f_t}{\pi c \delta^4} = \frac{f_t}{2E} \tag{17}$$

The degradation curve is based on an energy equivalence principle, allowing the use of softening curves obtained from experiments or other numerical models. In

Eq. (15), the ultimate stretch $s_u$ is a key parameter related to the fracture energy $G_f$. According to [6], the energy dissipated by all bonds crossing the fracture surface during the degradation process is assumed to equal $\xi w_d$, in which $w_d$ is the area under the degradation curve shown in Figure 1. The total energy dissipated per unit fracture area is equal to the fracture energy $G_f$. Thus, $w_d$ can be determined analytically in 3D through the following integral:

$$G_f = \int_0^{\delta} dz \int_0^{2\pi} d\theta \int_z^{\delta} d\xi \int_0^{\cos^{-1}(z/\xi)} w_d \xi^3 \sin\phi d\phi \tag{18}$$

and the solution is:

$$w_d = \frac{5G_f}{\pi\delta^5} \tag{19}$$

Then, the ultimate stretch is obtained by:

$$s_u = \frac{w_d}{f_{\max}} + s_0 \tag{20}$$

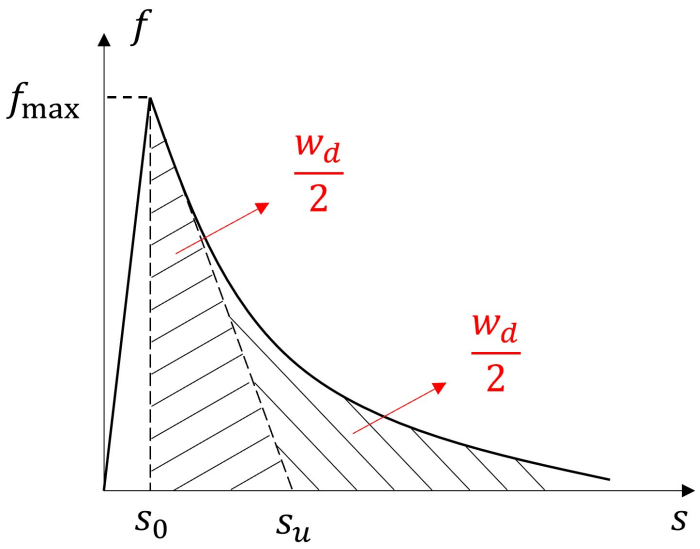


Figure 1: The proposed quasi-brittle damage model in BBPD

The above damage model provides a more realistic description of quasi-brittle failure and enables the incorporation of material fracture energy in the PD framework.

# 5 Numerical example

In this section, an experimental benchmark involving a three-point bending (TPB) test on a notched concrete beam is used to verify the peridynamic model with the proposed damage formulation. The experiment was reported in [15], and the corresponding

setup is shown in Figure 2. The load is applied at the top mid-span. In the numerical model, the load is applied through displacement control, with a maximum value of 0.5 mm. Therefore, a displacement control method, similar to the Newton–Raphson approach, is used to solve the nonlinear problem. The material properties used in this example are listed in Table 1.

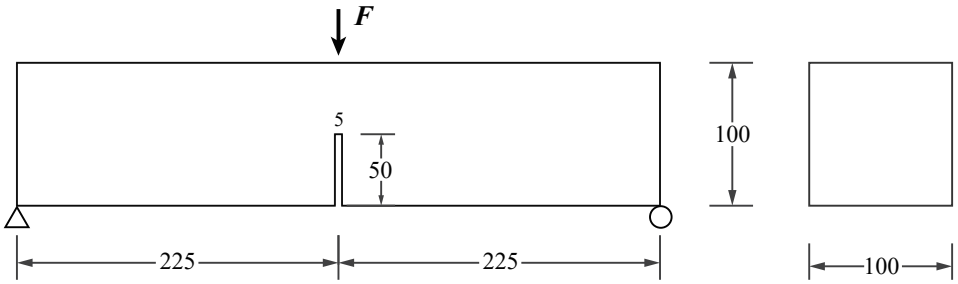


Figure 2: Geometry and boundary conditions of the notched TPB concrete beam (Unit: mm)

| Properties | Symbols | Units | Values |
|---|---|---|---|
| Young's modulus | $E$ | GPa | 20 |
| Poisson's ratio | $v$ | - | 0.25 |
| Tensile strength | $f_t$ | MPa | 2.4 |
| Fracture energy | $G_f$ | N/m | 90 |

Table 1: Material properties for notched TPB concrete beam

To reduce computational cost, only the mid-span region is modeled using 3D PD, while the remaining regions are modeled using CUF-based beam elements, as shown in Figure 3. Since the crack is expected to localize in the notched mid-span region, the proposed damage model is applied only in the 3D PD region. A linear elastic material model is used for the remaining parts. The coupling approach between PD and CUF-based beam elements follows the method described in [].

Table 2 lists the three numerical models used to study the influence of PD grid spacing. A smaller grid spacing leads to a larger number of PD particles. The horizon radius $\delta$ is taken as three times the grid spacing. In all models, eight second-order CUF-based beam elements are used.

The crack propagation of Model 1 is shown in Figure 4. A vertical crack initiates from the bottom notch and propagates upward. The damage index $\varphi$ for each particle is shown at different loading steps. This index represents the percentage of broken bonds around a particle. At a displacement of 0.1 mm, which corresponds to the peak

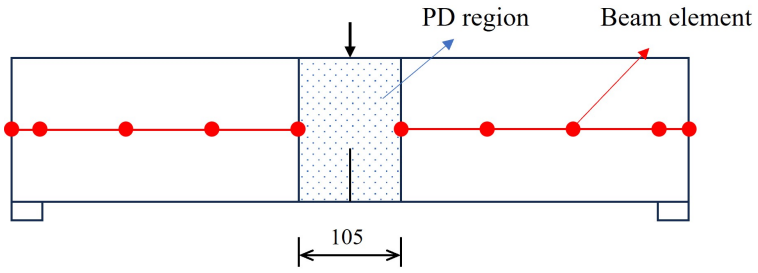


Figure 3: PD region and CUF-based beam element assignment

| Model No. | $\Delta x$ (mm) | $\delta$ (mm) | PD DoFs | FEM DoFs |
|---|---|---|---|---|
| Model 1 | 5 | 15 | 29,232 | 1,530 |
| Model 2 | 2.5 | 7.5 | 216,972 | 1,530 |
| Model 3 | 4 | 12 | 52,884 | 1,530 |

Table 2: Model information for notched TPB concrete beam

load, the damage is still limited. After that point, the crack grows rapidly and becomes clearly visible.

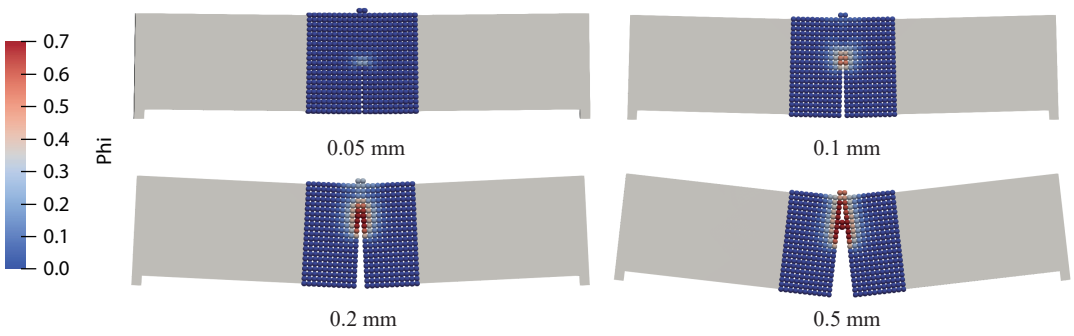


Figure 4: Crack propagation and damage index $\varphi$ evolution of Model 1 (Sacle factor=50)

The load–displacement curves at the mid-span for all three models are shown in Figure 5, along with experimental data for comparison. All numerical models show identical linear stiffness, which agrees well with the experimental results. The peak loads and post-peak softening behavior of the models also fall within the experimental range. Slight variations in peak loads and corresponding displacements are observed. These differences are likely due to slight variations in the location of the PD particles used to extract displacement. It is also evident that reducing the grid spacing significantly increases the number of degrees of freedom (DoFs), but the numerical

performance remains similar across all models.

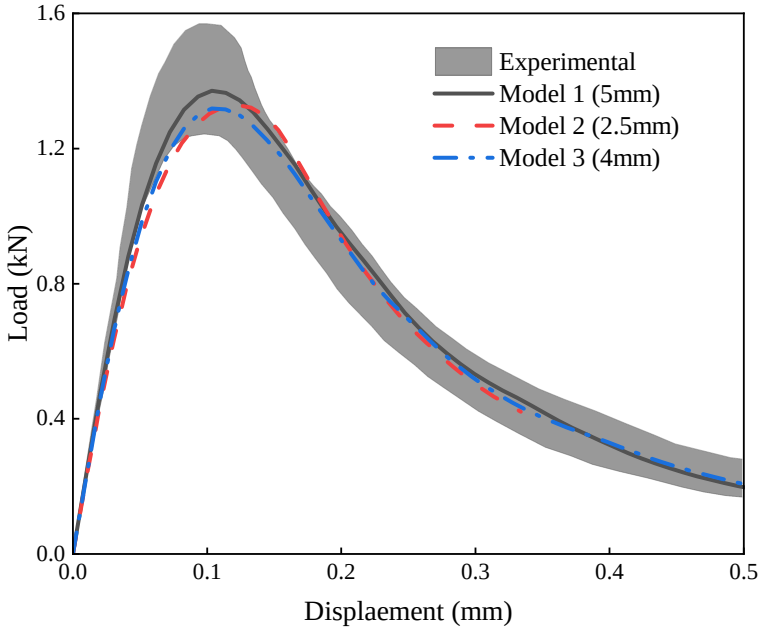


Figure 5: Comparisons of experimental and numerical load-displacement curves

# 6 Conclusions

This work proposed an improved damage model and implemented it in an existing PD–FEM coupled framework for the failure analysis of quasi-brittle materials. The coupling was achieved between 3D PD grids and CUF-based 1D finite elements using Lagrange multipliers. In the proposed damage model, bond stretch serves as the criterion for damage initiation, while the subsequent degradation is considered based on an energy-equivalence principle. With this model, the coupled PD–FEM system can successfully capture the crack propagation in a notched concrete beam under three-point bending. In addition, it accurately reproduces the structural load–displacement response, showing good agreement with experimental results. Moreover, the model shows consistent results across different grid sizes, confirming its numerical robustness.

## Acknowledgements

This project has received funding from the European Research Council (ERC) under the European Union's Horizon 2020 research and innovation programme (Grant agreement No. 850437). The authors are also thank full for the support provided by

the research projects 0305/1102/24160 MESTR - Modelação do Comportamento Estrutural a 0302/1102/24163 SEPINOV - Sistemas Estruturais e Produtos Inovadores from LNEC.

# References

[1] Z. P. Bažant and B. H. Oh, "Crack band theory for fracture of concrete," *Matériaux et construction*, vol. 16, pp. 155–177, 1983.

[2] M. Elices, G. Guinea, J. Gomez, and J. Planas, "The cohesive zone model: advantages, limitations and challenges," *Engineering fracture mechanics*, vol. 69, no. 2, pp. 137–163, 2002.

[3] S. A. Silling, "Reformulation of elasticity theory for discontinuities and long-range forces," *Journal of the Mechanics and Physics of Solids*, vol. 48, no. 1, pp. 175–209, 2000.

[4] A. Javili, R. Morasata, E. Oterkus, and S. Oterkus, "Peridynamics review," *Mathematics and Mechanics of Solids*, vol. 24, no. 11, pp. 3714–3739, 2019.

[5] S. A. Silling and E. Askari, "A meshfree method based on the peridynamic model of solid mechanics," *Computers & structures*, vol. 83, no. 17-18, pp. 1526–1535, 2005.

[6] D. Yang, W. Dong, X. Liu, S. Yi, and X. He, "Investigation on mode-i crack propagation in concrete using bond-based peridynamics with a new damage model," *Engineering Fracture Mechanics*, vol. 199, pp. 567–581, 2018.

[7] D. Yang, X. He, S. Yi, and X. Liu, "An improved ordinary state-based peridynamic model for cohesive crack growth in quasi-brittle materials," *International Journal of Mechanical Sciences*, vol. 153, pp. 402–415, 2019.

[8] W. Liu and J.-W. Hong, "A coupling approach of discretized peridynamics with finite element method," *Computer methods in applied mechanics and engineering*, vol. 245, pp. 163–175, 2012.

[9] Y. Bie, X. Cui, and Z. Li, "A coupling approach of state-based peridynamics with node-based smoothed finite element method," *Computer Methods in Applied Mechanics and Engineering*, vol. 331, pp. 675–700, 2018.

[10] A. Pagani and E. Carrera, "Coupling three-dimensional peridynamics and high-order one-dimensional finite elements based on local elasticity for the linear static analysis of solid beams and thin-walled reinforced structures," *International Journal for Numerical Methods in Engineering*, vol. 121, no. 22, pp. 5066–5081, 2020.

[11] E. Carrera, M. Cinefra, M. Petrolo, and E. Zappino, *Finite element analysis of structures through unified formulation*. John Wiley & Sons, 2014.

[12] A. Pagani, M. Enea, and E. Carrera, "Quasi-static fracture analysis by coupled three-dimensional peridynamics and high order one-dimensional finite elements based on local elasticity," *International Journal for Numerical Methods in Engineering*, vol. 123, no. 4, pp. 1098–1113, 2022.

[13] M. Arruda, J. Pacheco, L. M. Castro, and E. Julio, "A modified mazars damage model with energy regularization," *Engineering Fracture Mechanics*, vol. 259, p. 108129, 2022.

[14] J. Shen, M. T. Arruda, and A. Pagani, "Concrete damage analysis based on higher-order beam theories using fracture energy regularization," *Mechanics of Advanced Materials and Structures*, vol. 30, no. 22, pp. 4582–4596, 2023.

[15] H. Kormeling and H. Reinhardt, "Determination of the fracture energy of normal concrete and epoxy modified concrete," *Delft University of Technology, Report*, pp. 5–83, 1983.